Current-dependent Inactivation Induced by Sodium Depletion in Normal and Batrachotoxin-treated Frog Node of Ranvier

JEAN-MARC DUBOIS and ALAIN COULOMBE

From the Laboratoire de Neurobiologie, Ecole Normale Supérieure, 75230, Paris Cedex 05, and the Laboratoire de Physiologie Comparée, Université Paris-XI et de Physiologie Cellulaire et des Ensembles Neuronaux, Associé au CNRS, 91405 Orsay Cedex, France

ABSTRACT In batrachotoxin (BTX)-treated frog node of Ranvier, in spite of a marked reduction in Na inactivation, the Na current still presents a time- and voltage-dependent inactivation that could induce a 50–60% decrease in the current. The inactivation was found to be modified by changing the amplitude of a conditioning pulse, adding tetrodotoxin in the external solution, or replacing NaCl with KCl in the external solution. Conditioning pulses were able to alter the reversal potential of the BTX-modified Na current (V_{rev}). V_{rev} was shifted toward negative values for inward conditioning currents and was shifted toward positive values for outward conditioning currents. The change in V_{rev} was proportional to the conditioning current amplitude. Large inward currents induced 15–25-mV shifts of V_{rev}. During a 10–20-ms depolarizing pulse, the inactivation and change in V_{rev} were proportional to the time integral of the current. For longer depolarizations, V_{rev} reached a steady state level proportional to the current amplitude. The conductance, as calculated from the current and the actual V_{rev}, showed an inactivation proportional to $\exp(V_{rev} F/RT)$. These observations suggest that the BTX-modified Na current induces a decrease in local Na concentrations, which results in an alteration of the driving force and the conductance. During a pulse that induced a large inward current, the Na space concentration ($[Na]_s$) changed from 114 to 50–60 mM. In normal fibers, the reversal potential of Na current was also shifted toward negative values by a prepulse that induced a large inward current. The change in V_{rev} reached 5–15 mV, which corresponded to a decrease in $[Na]_s$ of 20–50 mM. This change in V_{rev} slightly altered the time course of Na current. On the basis of a three-compartment model (axoplasm-perinodal space-bulk solution), a Na permeability of the barrier between the space and the bulk solution ($P_{Na,s}$) and a mean thickness of the space (θ) were calculated. The mean value of $P_{Na,s}$ was 0.0051 $cm \cdot s^{-1}$ in both normal and BTX-treated fibers, whereas the value of θ was 0.29 μm in BTX-treated fibers and 0.05 μm in normal fibers. When

Address reprint requests to Dr. Jean-Marc Dubois, Laboratoire de Physiologie Comparée, Université Paris XI, Bât. 443, 91405 Orsay Cedex, France.

J. GEN. PHYSIOL. © The Rockefeller University Press · 0022-1295/84/07/0025/24$1.00 25

Volume 84 July 1984 25–48

compared with the values calculated during K accumulation, $P_{Na,s}$ was 10 times smaller than $P_{K,s}$ and $\theta_{Na\text{-}BTX}$ was equal to θ_K. Finally, it was shown by computer simulations that during a single action potential or a train of action potentials, $[Na]_s$ can decrease from 114 to 100–90 mM. However, neither the shape nor the amplitude of the action potentials was significantly modified by the decrease in $[Na]_s$.

INTRODUCTION

It is now well established that in many different biological tissues, ionic currents underlying the electrical excitability induce transient changes in local ionic concentrations. An accumulation of K ions in restricted pericellular spaces or in clefts between adjacent cells has been demonstrated from K current recordings under voltage clamp in squid giant axon (Frankenhaeuser and Hodgkin, 1956; Adelman et al., 1973), frog node of Ranvier (Dubois and Bergman, 1975; Moran et al., 1980; Dubois, 1981*a*; De Bruin, 1982), cardiac cells (Noble, 1976; Baumgarten and Isenberg, 1977; Cleemann and Morad, 1979*a*, *b*), skeletal muscle cells (Adrian et al., 1970), and molluscan neurons (Baylor and Nicholls, 1969). Changes in external K concentration during electrical activity were also directly measured using K-selective microelectrodes in snail neurons (Neher and Lux, 1973), cardiac cells (Kline et al., 1980; Cohen and Kline, 1982), rat optic nerve (Connors et al., 1982), and mammalian central nervous system (see review by Somjen, 1979). An accumulation of Na ions has been reported in the axoplasm of voltage-clamped myelinated nerve fibers submitted to repetitive depolarizations (Bergman, 1970). From current noise analyses in the node of Ranvier, Neumcke and Stämpfli (1983) have suggested that an inward Na current could induce a depletion of Na ions at the external surface of the membrane. From these observations, it appears that transient changes in local ionic concentrations during electrical activity may induce noticeable modifications in the characteristics of ionic currents and in cell activity. These modifications include changes in ionic driving forces and consequently in the excitability of cells, and also changes in metabolism (see reviews by Somjen, 1979; Pentreath, 1982).

In the present paper, we study the effects of Na current-induced local Na concentration changes on Na current and Na conductance in batrachotoxin (BTX)-treated and normal frog nodes of Ranvier. In normal voltage-clamped nodes of Ranvier, the Na current inactivates in a few milliseconds. Consequently, the total quantity of charges transported by the Na current is relatively small. After modification of Na channels by BTX, the Na inactivation is almost completely removed (Khodorov et al., 1975; Khodorov and Revenko, 1979). Under these conditions, a large quantity of Na ions enters the fiber during a maintained voltage step, and it can be expected that the local Na concentrations are noticeably altered by this current. We present several arguments in favor of the view that the local Na concentrations are indeed modified by Na currents, not only in BTX-treated nodes but also in normal nodes of Ranvier.

METHODS

Experiments were carried out on isolated, myelinated nerve fibers from the frog *Rana*

esculenta. Membrane currents were recorded under voltage-clamp conditions using the method of Nonner (1969). The resting potential of normal fibers (−70 mV) was defined as the potential at which 30% fast Na inactivation occurred. The resting Na inactivation was removed by a 50-ms pulse to −110 mV. In BTX, the holding potential was −120 mV, a potential at which all Na-modified channels were closed. Linear capacitative and ionic currents were analogically subtracted from the total current. The series resistance was not compensated for. Possible effects of series resistance were disregarded (see Chiu, 1977; Dubois and Schneider, 1981). The Ringer's solution contained (in mM): 111.5 NaCl, 2.5 KCl, 1.8 $CaCl_2$, 2.4 $NaHCO_3$, pH 7.4. Currents through K channels were blocked by replacing the end-pool solution by 120 mM CsF and adding 10 mM tetraethylammonium to the external solution. The method of BTX treatment was as described previously (Dubois et al., 1983).

RESULTS

Change in Ionic Driving Force During Voltage Pulses

Fig. 1 presents a family of inward and outward membrane currents recorded on a BTX-treated fiber during and after voltage pulses of various amplitudes. After activation, the current declines to a steady state level in ~20 ms. This decrease in current has been attributed both to a partial inactivation of the conductance and to a change in the selectivity of the channels during the voltage pulses (Mozhaeva et al., 1981). However, considering the large quantity of ionic charges transported during the pulses from one side of the membrane to the other, one cannot ignore the possibility of changes in local Na concentrations induced by inward Na currents. In order to test this possibility, the current was recorded near its reversal potential without and with a predepolarization (Fig. 2). In Fig. 2, *a* and *d*, the current was recorded during a pulse to +35 mV. In the experiment presented, this value corresponded to the reversal potential of the current, which consequently was nil during the depolarization. However, when a predepolarization was applied, the current during the pulse to +35 mV became outward after a prepulse to −60 mV, which induced an inward current (Fig. 2, *b* and *c*), and it became inward after a prepulse to +100 mV, which induced an outward current (Fig. 2, *e* and *f*). Moreover, the current at +35 mV increased with the duration of the predepolarization.

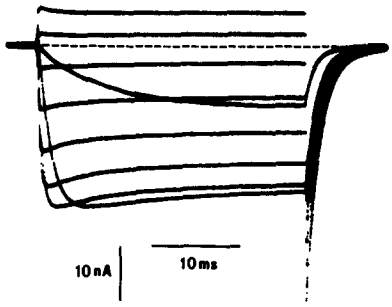

FIGURE 1. Ionic currents through BTX-modified Na channels. Family of currents in response to depolarizations from a holding potential of −120 mV to various potentials in 20-mV increments. Temperature, 11°C. Fiber 26-11-81.

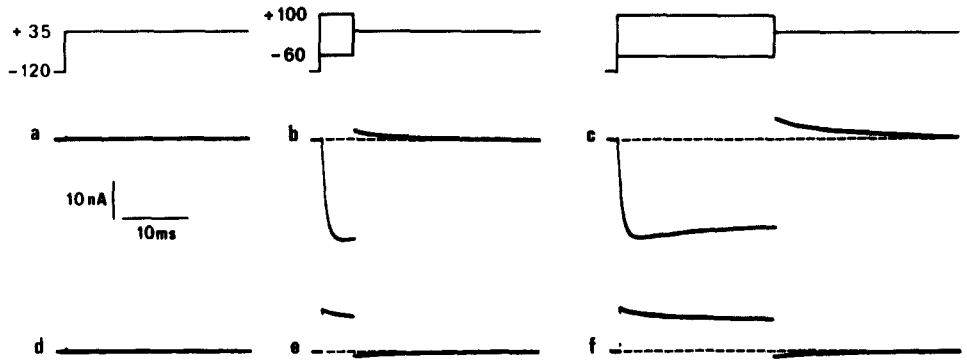

FIGURE 2. Change in reversal potential of BTX-modified Na current. (*a* and *b*) The current was recorded during a depolarization to +35 mV, which corresponded to the reversal potential. (*b* and *c*) The depolarization to +35 mV was preceded by a conditioning pulse to −60 mV. (*e* and *f*) The depolarization to +35 mV was preceded by a conditioning pulse to +100 mV. Temperature, 12°C. Fiber 25-11-81.

Steady State Na Inactivation

In BTX-treated fibers, the steady state Na inactivation has been studied from instantaneous tail currents arising after a large and short test pulse, which was preceded by long conditioning pulses of various amplitudes (Mozhaeva et al., 1981). Using such a protocol, the steady state inactivation of the current decreases to ~0.7–0.5 near −70 mV and then increases again for more positive conditioning depolarizations. This has been attributed to transitions of the channels to an inactivated state (h_1) and then to a second open state (h_2) (Mozhaeva et al., 1981). In Fig. 3, the relative amplitude of the initial tail current after the test pulse and the amplitude of the current at the end of the conditioning pulse

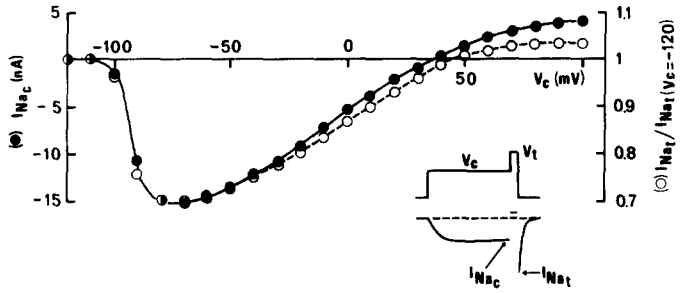

FIGURE 3. Steady state current and current inactivation-voltage curves of a BTX-treated fiber. Inset: pulse protocol used and corresponding currents. The conditioning current ($I_{Na,c}$) was measured at the end of 50-ms conditioning pulses (V_c) of various amplitudes. The test current ($I_{Na,t}$) was the quasi-instantaneous current recorded upon repolarization to −120 mV after a 1-ms test pulse V_t to +80 mV. $I_{Na,c}$ (filled circles) and $I_{Na,t}$, relative to its value in the absence of V_c (V_c = −120 mV) (open circles), are represented against the amplitude of V_c. Temperature, 13°C. Fiber 13-10-82.

have been plotted against the conditioning voltage. The relative amplitude of the test current (open circles) decreased to 0.7 at −70 mV and then rose again as the conditioning voltage was made increasingly positive. For conditioning voltages larger than +50 mV, the initial tail current was larger than in the absence of prepulse. This could indicate that inactivation was present even at −120 mV. However, it appears that both the amplitude of the current measured

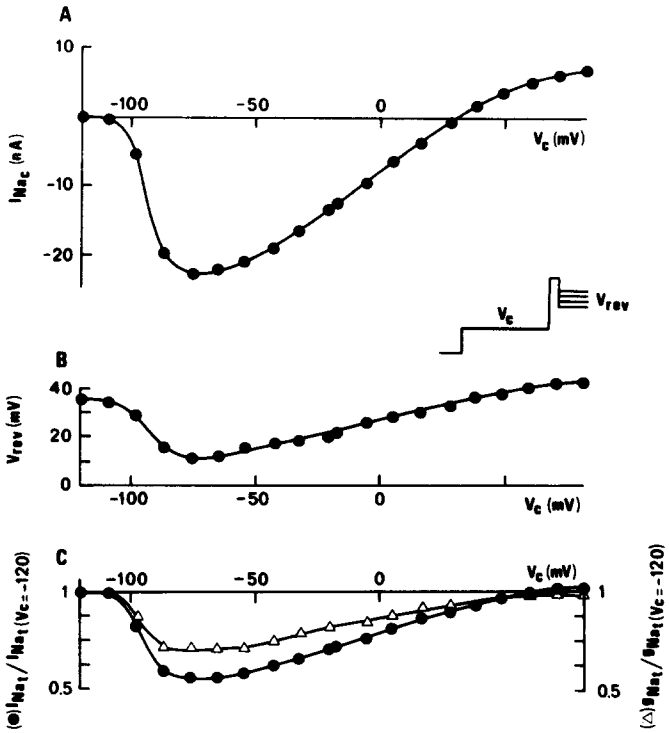

FIGURE 4. Current, reversal potential, and inactivation-voltage curves in a BTX-treated fiber. (*A*) Conditioning current-voltage curve. The conditioning current was measured at the end of 50-ms conditioning pulses of various amplitudes. (*B*) Reversal potential of the current as a function of the conditioning pulse amplitude. The reversal potential was determined as shown in the inset by a third pulse of various amplitudes applied at the end of a 0.5-ms test pulse to +80 mV. (*C*) Relative test current (filled circles) determined as in Fig. 3 and relative test conductance (open triangles) as a function of the conditioning pulse amplitude. The conductance was calculated from the test current and the actual reversal potential. Temperature, 12°C. Fiber 25-11-81.

at the end of the conditioning pulse and the inactivation of the tail current after the test pulse change similarly. If the ionic flux during the conditioning pulse alters the ionic driving force, one can interpret this kind of current inactivation as being directly related to changes in driving force induced by the current itself.

In the experiment presented in Fig. 4, the current at the end of conditioning pulses of various amplitudes and the initial tail current after the test pulse were

measured as above, and the actual reversal potential of the current was determined at the end of the test pulse. Then, the conductance at the end of the test pulse was calculated from the initial tail current and the actual reversal potential. One can see that the reversal potential of the current is markedly altered by the conditioning current, since after a prepulse to −75 mV, for which the inward conditioning current is maximum, the reversal potential is 25 mV more negative than in the absence of conditioning current. As a consequence of the change in driving force induced by the conditioning current, the test current (initial tail current) is altered. However, it is important to note that the conductance at the end of the test pulse is also affected by the conditioning pulse in the same way as the test current and the reversal potential.

In normal frog node of Ranvier and squid giant axon, it has been shown that the Na conductance is dependent on external and internal Na concentrations (Dubois and Bergman, 1971; Landowne and Scruggs, 1981; Fig. 13 of the present paper). If, in BTX-treated nodes of Ranvier, the conductance can be altered by rapid changes in local Na concentrations, the inactivation of the conductance can be directly related to changes in local Na concentrations induced by the Na current. The results presented in Fig. 5 confirm this hypothesis.

The ionic selectivity of BTX-modified Na channels is smaller than that of normal Na channels (Khodorov and Revenko, 1979). Under the conditions of the present experiments, one can assume, to a first approximation, that the current through BTX-modified channels is exclusively transported by external Na and internal Cs. The reversal potential of the net current (V_{rev}) is expressed by Eq. 1 (Goldman, 1943; Hodgkin and Katz, 1949):

$$V_{rev} = \frac{RT}{F} \ln \frac{P_{Na}\,[Na]_o}{P_{Cs}\,[Cs]_i}, \tag{1}$$

where P_{Na} and P_{Cs} are the permeabilities of the channels to Na and Cs, $[Na]_o$ and $[Cs]_i$ are the actual external Na and internal Cs concentrations, T is the temperature, and R and F are the usual constants. An inward Na current may induce an internal accumulation of Na ions and an outward Cs current may induce an external accumulation of Cs ions. In these cases, $P_{Na}\,[Na]_i$ and $P_{Cs}\,[Cs]_o$ must be introduced in Eq. 1. If the change in V_{rev} is due to a change in local concentrations, $\exp V_{rev}F/RT$ must be strictly related to the quantity of charges (i.e., the time integral of the current) transported during the conditioning pulse. However, it appears from Figs. 8 and 9*A* that during a maintained depolarization, V_{rev} and I_{Na} (and consequently the change in local concentrations) reach a steady state level in 10–20 ms. Therefore, the change in local concentrations would be more likely to be related to the amplitude of the current at the end of the 50-ms conditioning pulses than to the time integral of the conditioning current. This hypothesis is confirmed by the results in Fig. 5*A*, which show a proportionality between the change in V_{rev} and the amplitude of the current measured at the end of the conditioning pulse. Fig. 5*B* represents the change in conductance calculated from initial tail currents as a function of $\exp V_{rev}F/RT$ [i.e., from Eq. 1: $(P_{Na}\,[Na]_o)/(P_{Cs}\,[Cs]_i)$]. The results show a direct relation between the change

in conductance and the change in local concentrations (as expressed by $\exp V_{rev}F/RT$), as expected if the conductance is modulated by the current via changes in local concentrations of permeant ions.

Steady State Inactivation After Pharmacological Reduction of the Current

In the preceding section, it was concluded that the apparent inactivation of the test current was different from the classical process of channel inactivation and was in fact related to the conditioning current, which induced changes in both the ionic driving force and conductance. In these experiments, the amplitude of the conditioning current was changed by changing the conditioning voltage. It

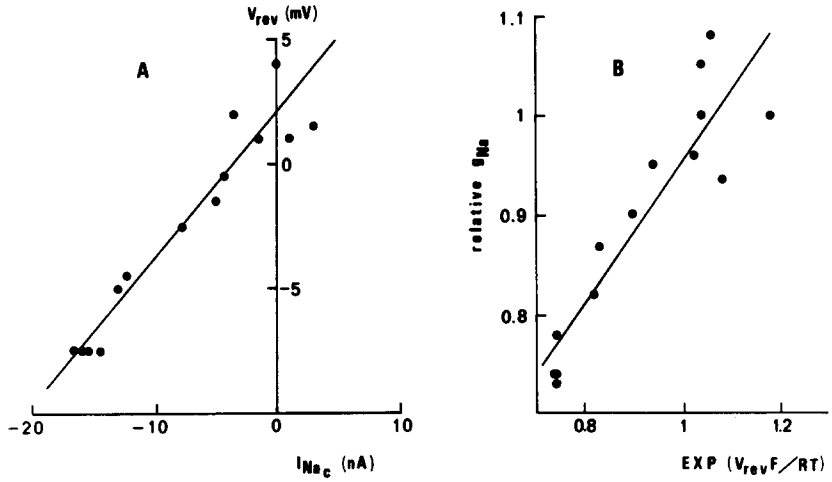

FIGURE 5. Relationship between current, reversal potential, and conductance of BTX-modified Na channels. (*A*) Reversal potential as a function of the conditioning current. The conditioning current was measured at the end of 50-ms conditioning pulses of various amplitudes. The reversal potential was determined as in Fig. 4 after a 1-ms test pulse to +10 mV. (*B*) Relative conductance as a function of the concentration gradient $(P_{Na}[Na]_s)/(P_{Cs}[Cs]_i) = \exp(V_{rev}F/RT)$. The conductance was calculated as in Fig. 4. The straight lines were obtained by linear regression to the data points. Temperature, 13°C. Fiber 13-11-81.

was of interest to see whether pharmacological manipulations that induced a decrease in the current amplitude would also decrease the inactivation of the test current and the change in reversal potential after the conditioning pulses. In the following experiments, the current was reduced by replacement of external NaCl by KCl or addition of tetrodotoxin to the external solution. BTX-modified channels are permeable to K with a ratio $P_K/P_{Na} = 0.4$ (Khodorov and Revenko, 1979). Consequently, after replacement of external NaCl by KCl, the inward current must be decreased and the outward current increased. Fig. 6*A* presents traces of current recorded at −60 and +60 mV in Na solution (control solution), in K solution, and in Na solution with 10^{-8} M of tetrodotoxin (TTX). When compared with the traces in control solution, the decline in current during the

pulses is smaller at −60 mV in K solution and at −60 and +60 mV in Na solution plus TTX, but it is larger at + 60 mV in K solution, as would be expected from the depletion-accumulation hypothesis. Indeed, the inward current at −60 mV in K solution and Na solution plus TTX and the outward current at +60 mV in Na solution plus TTX are smaller than in control solution. In contrast, because of the smaller permeability of the channels to K than to Na ions, the outward current at +60 mV in K solution is larger than in control solution.

The steady state inactivation of the test current was calculated in each solution using the protocol in Fig. 3 and was plotted against the conditioning voltage (Fig. 6*B*). It appears that the relative current is larger in K and Na plus TTX solutions than in control solution, especially for conditioning voltages more

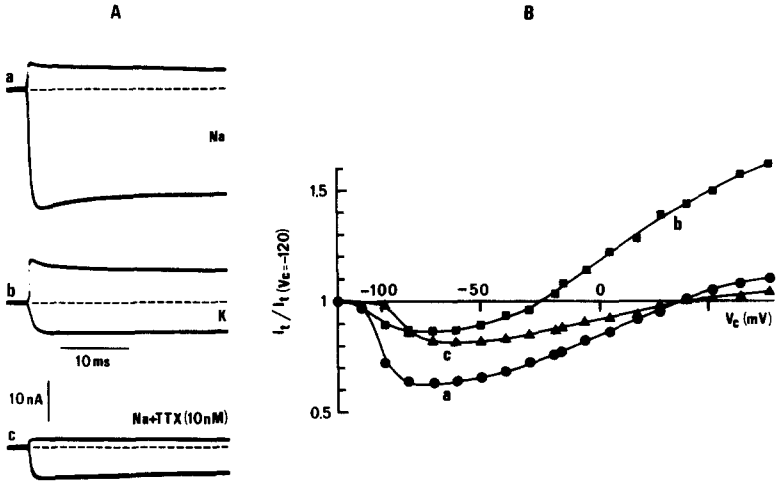

FIGURE 6. Effect of current reduction on the steady state current inactivation in a BTX-treated fiber. (*A*) Superimposed traces of current recorded during depolarizations to −60 and +60 mV in Na Ringer's (*a*), K Ringer's (*b*), and Na Ringer's plus 10 nM TTX (*c*). (*B*) Relative test current as a function of conditioning pulse amplitude in Na Ringer's (circles), K Ringer's (squares), and Na Ringer's plus 10 nM TTX (triangles). The test current was recorded as in the preceding figures after a 1-ms test pulse to +40 mV. Temperature, 11°C. Fiber 26-11-81.

positive than −20 mV. This may be due to an accumulation of permeant ion at the external face of the membrane or to a decrease in the permeant ion concentration at the inner face of the membrane resulting from the large outward conditioning current. The reduction in steady state inactivation observed in the presence of TTX can be interpreted as being directly related to a smaller accumulation-depletion of permeant ions if toxin does not by itself alter the inactivation or the selectivity of the channels. This conclusion is confirmed by the observation that the change in the reversal potential of the current induced by a conditioning pulse to −60 mV is also reduced by TTX (10^{-8} M), which decreases the conditioning current to ~20% of its control value (Table I).

These observations suggest that the inactivation of the current is due only to

changes in ionic driving force induced by the current. If this is true, no inactivation would develop when there is no current. This is very nearly the case at V_{rev} (see Figs. 3 and 4); however, one cannot exclude the existence of several current components with different reversal potentials (see Dubois et al., 1983, and Discussion).

Another way to abolish the current is to block the channels completely with TTX. Of course, under these conditions, it becomes impossible to test the inactivation directly. However, the inactivation in the absence of current can be deduced from extrapolation of the relation "inactivation of the test current vs.

TABLE I

Shift of Na Reversal Potential and Decrease in [Na]$_s$ Induced by an Inward Conditioning Current

BTX-treated fibers	ΔV_{rev}	$\Delta[Na]_s$	Normal fibers	ΔV_{rev}	$\Delta[Na]_s$
	mV	*mM*		*mV*	*mM*
25-11-81	−23	−69	12-6-78	−8	−32
3-12-81	−10	−39	14-6-78	−5	−21
7-12-81	−20	−63	16-6-78	−8	−32
16-12-81	−20	−63	19-6-78	−8	−32
11-10-82	−19	−61	20-6-78	−15	−52
12-3-83	−11	−41	22-6-78	−6	−25
Mean±SEM	−17±2	−56±5	14-3-83	−12	−44
			14-4-83	−7	−28
			4-5-83	−10	−38
			2-6-83	−9	−35
			Mean±SEM	−9±1	−34±3

BTX-treated fibers + 10 nM TTX	ΔV_{rev}	$\Delta[Na]_s$
	mV	*mM*
3-12-81	0	0
7-12-81	0	0
16-12-81	−3	−13
12-3-82	0	0
12-5-82	−3	−13
Mean±SEM	−1±1	−5±3

The reversal potential was determined with and without a 0.5- or 1-ms conditioning pulse to 0 or −10 mV on normal fibers, and with and without a 50-ms conditioning pulse to −60 mV on BTX-treated fibers. In TTX, the current was decreased to ~20% of its control value.

conditioning current" when the conditioning current is increasingly reduced by increased concentrations of TTX. This type of experiment was carried out by recording the test current in the absence and in the presence of a 50-ms conditioning pulse to −60 mV and recording the conditioning current at the end of the conditioning pulse during the action of TTX (10 nM) and during washout. Under these conditions, the complete effect of TTX develops within 5–10 min of switching to the new solution. During this period, test and conditioning currents were measured every 15 or 30 s. The relative test current was plotted against the amplitude of the conditioning current (Fig. 7). Except for a small deviation in the largest conditioning currents, the values are distributed

along a straight line, and extrapolation indicates that there is hardly any inactivation of the test current when there is no conditioning current. In three identical experiments, the extrapolation of the regression line to zero conditioning current gave relative test currents of 0.98, 1.11, and 0.94, respectively.

Kinetics of Inactivation

The preceding results suggest that in BTX-treated nodes of Ranvier, Na inactivation is related to changes in local Na concentrations. To further test this conclusion, we analyzed the simultaneous changes in Na current, conductance, and reversal potential during a voltage pulse. In the experiment presented in Fig. 8, the current was measured at the end of a first pulse to −60 mV of various

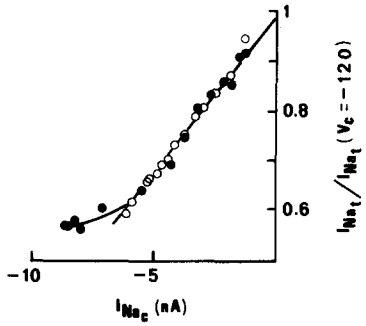

FIGURE 7. Steady state current inactivation as a function of the current amplitude modified by TTX in a BTX-treated fiber. The test current was recorded upon repolarization after a 0.5-ms pulse to +50 mV preceded or not by a 50-ms conditioning pulse to −60 mV. The conditioning current and pairs of test currents (with and without V_c) were recorded every 15 or 30 s during the application of 10 nM TTX (filled circles) and during washout (open circles). The straight line was obtained from a linear regression to all data points except those corresponding to the four largest $I_{Na,c}$. The extrapolation of the straight line to $I_{Na,c} = 0$ gives a relative $I_{Na,c}$ of 0.98. Temperature, 14°C. Fiber 21-7-82.

durations and the reversal potential of the current was determined with a second pulse. Then the conductance was calculated from the current and the actual reversal potential. After activation, both current and conductance show a decline that develops in parallel with the change in reversal potential. At this stage of the analysis, two points must be clarified: (*a*) Is the change in reversal potential related only to the inward Na current, or is it partly due to a change in selectivity of the channels (Mozhaeva et al., 1981)? (*b*) Is the decline in the conductance related only to a change in local Na concentrations? If the change in reversal potential were due only to a change in local Na concentrations induced by the influx of Na ions, it would be proportional to the quantity of Na ions leaving the nodal space to enter the fiber, i.e, to the time integral of the current. Fig. 9 shows that V_{rev} is indeed proportional to the time integral of current during the first 10 ms of depolarization. For a longer depolarization, V_{rev} does not change further but remains proportional to the amplitude of the current (see Fig. 5*A*).

This indicates that during a long depolarization, the local Na concentrations (outward and/or inward) change for a few milliseconds and then reach a steady state level that is proportional to the amplitude of the current. This justifies the relation used in Fig. 9*A* between V_{rev} and the amplitude of the current recorded at the end of 50-ms depolarizations.

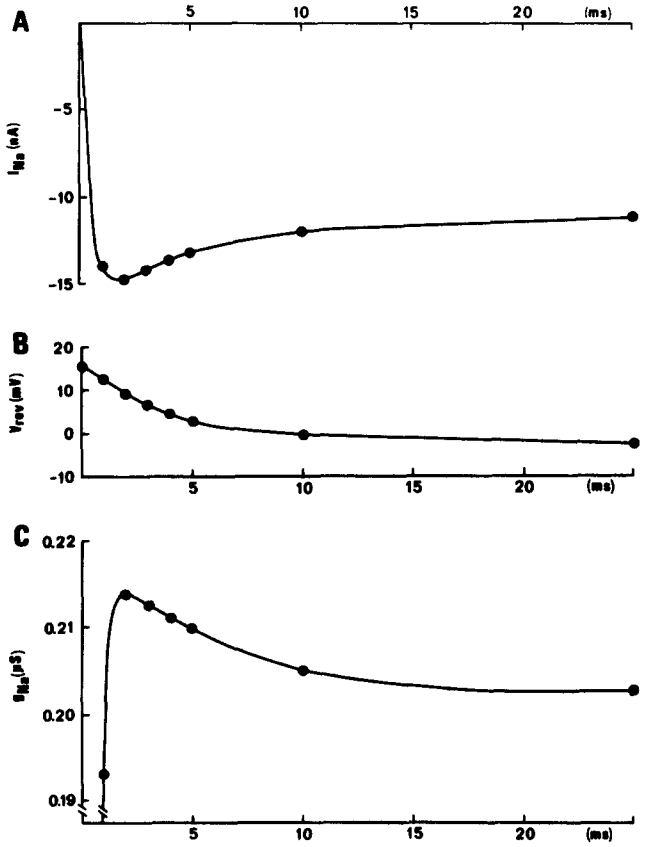

FIGURE 8. Na current, reversal potential, and conductance of a BTX-treated fiber as a function of time. (*A*) Current measured at the end of pulses of various durations to −60 mV. (*B*) Reversal potential of the current determined with a second pulse of various amplitudes. (*C*) Conductance calculated from the current and the actual reversal potential. Temperature, 13°C. Fiber 11-10-82.

Recovery of the Initial Local Na Concentrations

The recovery of the initial local Na concentrations was analyzed with a large test pulse applied at various times after a conditioning depolarization to −60 mV, which induced an inward Na current. Fig. 10 shows the variation of the peak tail current recorded at the end of a 1-ms test pulse vs. the time between the conditioning and the test pulses. Under these conditions, the relative amplitude of the peak tail current is proportional to the local Na concentrations, which

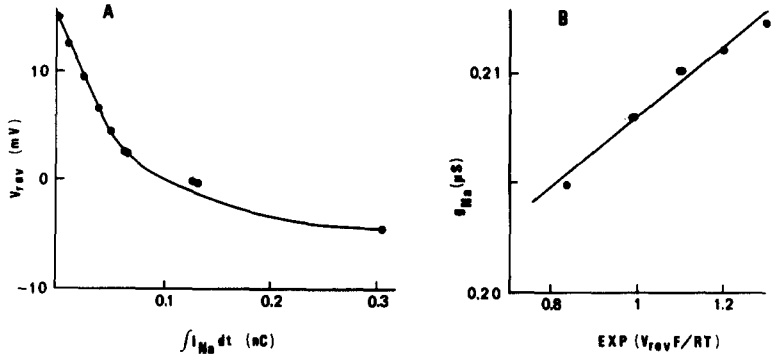

FIGURE 9. Relationship between time integral of Na current, reversal potential, and conductance in a BTX-treated fiber. (*A*) Reversal potential as a function of the quantity of entering Na ions during conditioning pulses (to −60 mV) of various durations. (*B*) Conductance as a function of the concentration gradient $(P_{Na}[Na]_s)/(P_{C_s}[C_s]_i) = \exp(V_{rev}F/RT)$. The conductance was calculated as in Fig. 4. Temperature, 13°C. Fiber 11-10-82.

have been altered by the current during the conditioning pulse and which return to their resting values. In this experiment, the peak tail current changes exponentially with a time constant of 16.5 ms. In another experiment, the time constant was found to be 19.0 ms.

Change in Local Na Concentrations in Normal Voltage-Clamped Fibers

If the environment of the membrane is not modified by BTX, it can be predicted from the preceding results that normal inward Na current must also induce

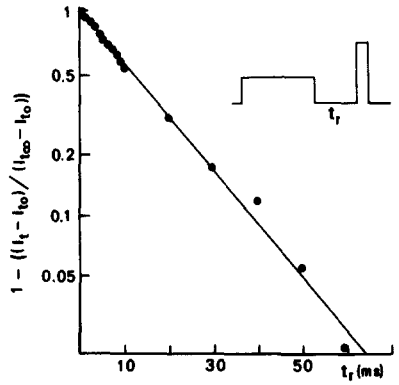

FIGURE 10. Kinetics of recovery of the initial Na concentrations in a BTX-treated fiber. The test current was recorded upon repolarization after a 0.5-ms pulse to +50 mV separated from a conditioning pulse (50 ms, −60 mV) by a gap of various durations (t_r). The inset gives the pulse protocol used. I_{t_0} and I_{t_∞} were, respectively, the test currents for $t_r = 0$ and $t_r = \infty$. The straight line was obtained from a linear regression to all data points. The time constant of the change in test current was 16.5 ms. Temperature, 14.5°C. Fiber 26-7-82.

changes in local Na concentrations. To test this, we studied fibers that had not been treated with BTX. I_{Na} was recorded during a depolarizing pulse near its reversal potential and then at the same voltage with a 0.5-ms prepulse to −10 mV, which induced a large peak of inward current. In the experiment in Fig. 11*A*, the reversal potential in the absence of prepulse was about +95 mV. After the prepulse, the current at +95 mV was clearly outward, and the instantaneous reversal potential was 12 mV more negative than in the absence of prepulse. Fig. 11*B* shows a similar change in reversal potential induced by a prepulse in another experiment. The peak I_{Na} is plotted against voltage in the absence and in the presence of a 1-ms prepulse to −10 mV, which shows the shift of the reversal potential induced by the prepulse to be −7 mV. Table I gives shifts of reversal potential induced by 0.5- or 1-ms prepulses to 0 or −10 mV in different fibers.

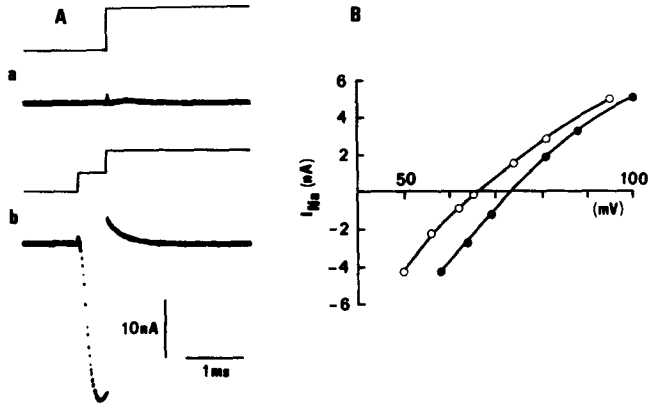

FIGURE 11. Change in reversal potential of Na current in a normal fiber. (*A*) Traces of Na current. (*a*) During a depolarization to +95 mV corresponding to the reversal potential. (*b*) The depolarization to +95 mV was preceded by a 0.5-ms conditioning pulse to −10 mV. Temperature, 14°C. Fiber 14-3-83. (*B*) Na current-voltage curves. The peak current was recorded during depolarizations of various amplitudes without a conditioning pulse (filled circles) and with a 1-ms conditioning pulse to −10 mV. Temperature, 14°C. Fiber 12-6-78.

In spite of some variability between fibers, a change in reversal potential was always noted with a mean shifted value ± SEM of 9 ± 1 mV. The variability between fibers is similar to that observed for the accumulation of K ions (Moran et al., 1980; Dubois, 1981*a*). This variability can be related to the amplitude of the current during the prepulse, the size of the node and of the paranodal space, or the nature of the fiber (motor or sensory), as also observed for K accumulation (Moran et al., 1980).

The question that immediately arises is whether the calculation of the conductance kinetic parameters gives noticeably different results when actual values of V_{rev} are used instead of a constant one. In the experiment in Fig. 12, the current was recorded during a pulse to −8 mV, and, at various times after the beginning of the pulse, the reversal potential of the current was determined

from an interpolation of the instantaneous current-voltage relationship. The conductance was then calculated at the same instant by using either an assumed constant reversal potential or the actual reversal potential. It appears that at its peak and during its inactivation phase, the conductance is slightly larger when calculated with the actual V_{rev} than when a constant V_{rev} was used. However, the difference can be considered negligible since the error in g_{Na} peak, activation, and inactivation time constants does not exceed 11%.

There remains the important question of whether the changes in V_{rev} induced by inward currents are due to a decrease in $[Na]_o$ rather than to an increase in $[Na]_i$ or to both. To answer this question, it is necessary to change the Na

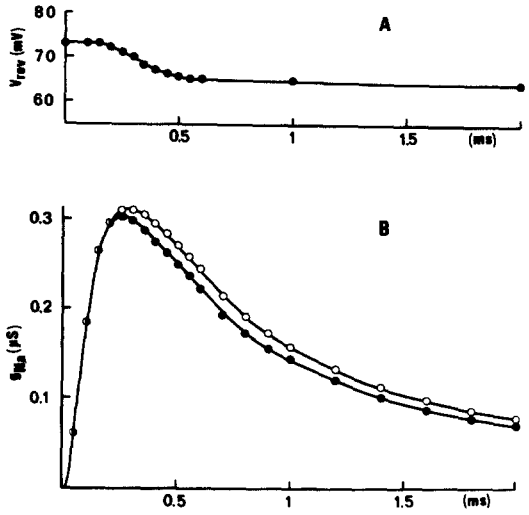

FIGURE 12. Reversal potential of Na current and conductance as a function of time in a normal fiber. (*A*) Reversal potential of the current determined with a second pulse of various amplitudes applied after a pulse to −8 mV of various durations. (*B*) Conductance as a function of time. The conductance was calculated from the current recorded at −8 mV and either a constant reversal potential determined without the pulse to −8 mV (filled circles) or the actual reversal potential (open circles). Temperature, 14°C. Fiber 12-6-78.

concentrations not only in the external solution but also in the axoplasm and to study the relations between Na concentrations and the conductance. In BTX-treated fibers, this type of experiment is complicated by the fact that BTX-modified channels are permeable to many cations that could be used as substitutes for Na. For this reason, experiments of this kind are better performed in normal fibers, but extending the results to BTX-treated fibers requires the assumption that the relations between conductance and Na concentrations are qualitatively similar in both preparations. Fig. 13 presents peak Na current-voltage curves in the presence of two internal and two external Na concentrations. It is clear that the maximum conductance is increased either when the external or the internal Na concentrations are increased. This observation confirms the results of Dubois

and Bergman (1971) on the same preparation and those of Landowne and Scruggs (1981) on the squid axon. It can be concluded that the decrease in conductance observed during a pulse more negative than V_{rev} on BTX-treated nodes is due to a decrease in Na concentration at the external face of the membrane rather than to an increase in the axoplasmic Na concentration. Similarly, an outward current would induce an accumulation of permeant ions at the external face of the membrane.

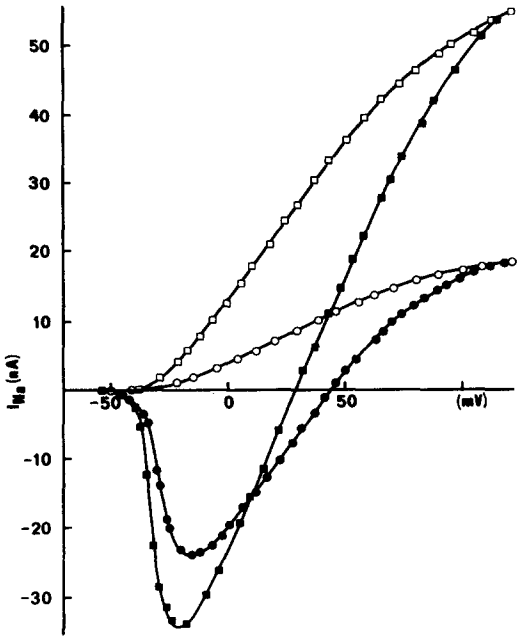

FIGURE 13. Na current-voltage curves in various external and internal Na concentrations. The peak Na current was recorded in external solutions containing either 114 (filled symbols) or 2.4 mM Na (open symbols), and in internal solutions containing either 19 (circles) or 35 mM Na (squares). Internal Na concentrations were calculated from the steady state reversal potentials with the Nernst equation. $[Na]_i$ was modified by changing the Na concentration in the two side pools. Temperature, 8°C. Fiber 13-2-78.

Calculations of the Parameters of Na Depletion

The preceding results suggest that inward Na current induces a depletion of Na ions from the external face of the membrane. Assuming that this depletion takes place in a perinodal space delimited by the axolemma, the Schwann cells, and an apparent external barrier, it was analyzed in terms of the three-compartment model (Frankenhaeuser and Hodgkin, 1956) proposed for K accumulation in the squid giant axon and used for K accumulation in the node of Ranvier (Dubois and Bergman, 1975; Moran et al., 1980). In the framework of the three-compartment model, the change in ionic concentration is defined by $\delta[Na]_s$, the space thickness θ (distance between the nodal membrane and the bulk), and $P_{l,s}$,

the apparent permeability of the external barrier for I ions. For a conditioning pulse lasting from t_0 to t_1, the change in Na concentration in the space over the concentration in the bulk solution ($\delta[\mathrm{Na}]_s$) is given by the equation:

$$\delta[\mathrm{Na}]_s = \frac{(1/F)\int_{t_0}^{t_1} I_{\mathrm{Na}}dt - (t_{\mathrm{Na}}/F)\int_{t_0}^{t_1} I_{\mathrm{Na}}dt - P_{\mathrm{Na,s}}\int_{t_0}^{t_1} \delta[Na]_s dt}{\theta}, \quad (2)$$

where I_{Na} is the Na current in $\mathrm{A}\cdot\mathrm{cm}^{-2}$, assuming a nodal membrane surface of 50 $\mu\mathrm{m}^2$ (Nonner et al., 1975), and t_{Na} is the transport number for Na in the space given by $t_{\mathrm{Na}} = [\mathrm{Na}]_s/\Sigma$ ([cations]$_s$ + [anions]$_s$) at time t_1. Calculations of θ and $P_{\mathrm{Na,s}}$ were made from different experiments both with and without BTX. Table II presents these values and, for comparison, the values of θ and $P_{\mathrm{K,s}}$ calculated for K accumulation by Dubois and Bergman (1975) and Moran et al. (1980); also presented are values from experiments where θ and $P_{\mathrm{I,s}}$ were calculated on the same normal fibers for K accumulation and Na depletion. Table II also gives values of time constants of recovery to the normal concentration (τ) determined experimentally as in Fig. 10 or calculated from the ratio $\theta/P_{\mathrm{I,s}}$. The values presented in Table II show several interesting points. $P_{\mathrm{Na,s}}$, which is not significantly different with or without BTX, is ~10 times smaller than $P_{\mathrm{K,s}}$, and θ_{Na} is ~4 times smaller without BTX than with BTX, but with BTX it is similar to θ_{K}. Finally, experimental τ is similar to calculated τ. These results cannot be attributed to differences between fibers, since the same values were obtained in similar conditions by different authors. Moreover, the differences between θ_{Na}, P_{Na}, and θ_{K}, $P_{\mathrm{K,s}}$ were observed on the same fibers (see below). They suggest that the volume of the nodal gap is modulated by its ionic composition and that the permeability of the barrier is different for Na and K (see Discussion).

TABLE II

Mean Space Thickness (θ) During Na Depletion or K Accumulation and Apparent Barrier Permeabilities (P_s) for Na and K

	Na	NA (BTX)	K	K (Dubois and Bergman, 1975)	K (Moran et al., 1980)
θ (μm)	0.05	0.29	0.58	0.29	0.59
$P_{\mathrm{I,s}}$ (cm s^{-1})	0.0065	0.0023	0.021	0.019	0.015
τ_{cal} (ms)	1.7	16.2	2.9	1.5	3.9
τ_{exp} (ms)	—	17.7	4.1	1.3	—

Mean of values was obtained on two to four experiments.

The increase in the volume of the gap in BTX and during K accumulation can be due either to an increase in nodal surface related to a detachment of the myelin or to an increase in the gap thickness. Experiments in which all the external NaCl was replaced by KCl showed that the capacity current (and thus the nodal membrane surface) remained unchanged. This suggests that the increase in gap volume in BTX and during K accumulation is due only to an

increase in gap thickness or a change in space geometry (see Discussion). This conclusion was confirmed by calculations of θ and $P_{I,s}$ in two normal fibers both during Na depletion (the K current was blocked by 10 mM external TEA) and during K accumulation (the K current was recorded at the equilibrium potential for Na ions). In these two experiments, the mean values of θ_{Na} and $P_{Na,s}$ were 0.036 μm and 0.0089 cm·s^{-1}, and the mean values of θ_K and $P_{K,s}$ were 0.58 μm and 0.021 cm·s^{-1}. In these calculations, θ and $P_{I,s}$ are mean values determined for various time intervals ($t_1 - t_0$).

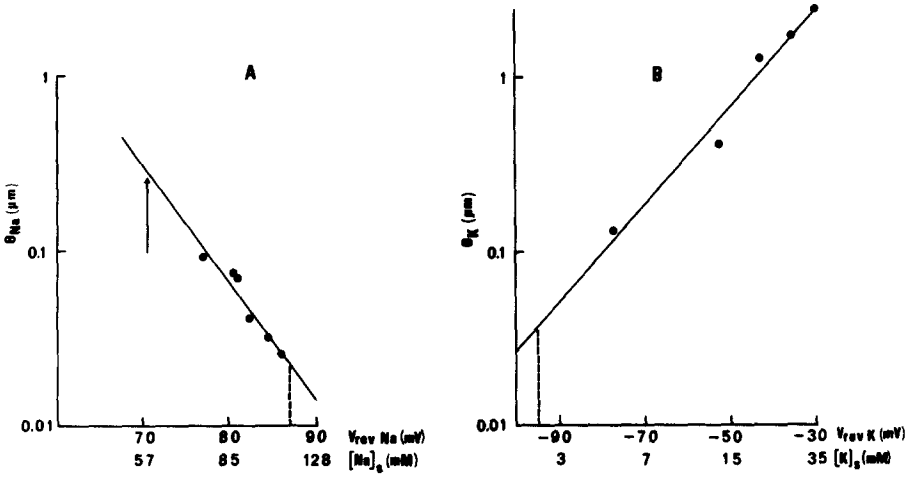

FIGURE 14. Relationships between the space thickness and the space ionic concentrations. The space thickness (θ) was calculated in a normal fiber from Eq. 1 either during Na depletion induced by an inward Na current elicited by a depolarization to 0 mV (*A*) or during K accumulation induced by an outward K current elicited by a depolarization to +87 mV (*B*). θ was calculated during different time intervals corresponding to different $[Na]_s$ and $[K]_s$. The dashed lines correspond to resting $[Na]_s$ and $[K]_s$, which are equal to their bulk concentrations. The arrow corresponds to the mean $[Na]_s$ calculated in BTX-treated fibers at the end of 50-ms depolarizations to −60 mV. K current was recorded at the reversal potential for Na ions and Na current was recorded in Ringer's solution +10 mM TEA. Temperature, 12°C. Fiber 4-5-83.

One explanation for the differences between θ_{Na}, $P_{Na,s}$ and θ_K, $P_{K,s}$ is that these parameters are functions of the Na and K concentrations in the space. In order to test this hypothesis, θ and $P_{I,s}$ were calculated for successive time intervals ($t_i - t_{i-1}$) corresponding to different Na and K concentrations in the space. The results show that $P_{Na,s}$ and $P_{K,s}$ are different and almost independent of ionic concentrations in the space. They confirm the view that the apparent barrier between the space and the bulk solution is somehow more permeable to K than to Na. In contrast, θ_K was found to increase when $[K]_s$ increased and θ_{Na} was found to increase when $[Na]_s$ decreased.

Fig. 14 represents the variation of θ_{Na} and θ_K with $[Na]_s$ and $[K]_s$, respectively,

in one typical fiber. From the results shown in this figure, three interesting points should be noted. (*a*) When exponential regressions are calculated through the points in Fig. 14, the extrapolation of the curve corresponding to the resting $[Na]_s$ (114 mM) and $[K]_s$ (2.5 mM) gives almost the same values for θ_{Na} (0.023 μm) and θ_K (0.036 μm). (*b*) The extrapolation of the $\theta_{Na} - [Na]_s$ curve to the mean $[Na]_s$ calculated in BTX gives a θ_{Na} value of 0.30 μm, which is very close to the θ_{Na} value calculated in BTX (see Table II). (*c*) The extrapolation of the $\theta_K - [K]_s$ curve to the isotonic $[K]_s$ (120 mM) gives a θ_K value of 16.2 μm. This indicates that in isotonic KCl Ringer's, θ would reach a value ~500 times its resting value in normal Ringer's solution. It would be of interest to test this

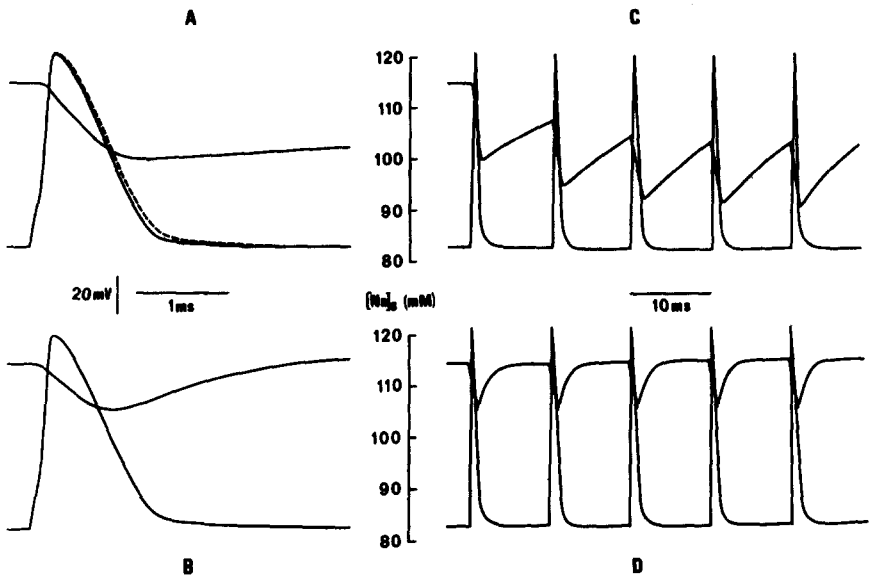

FIGURE 15. Computed action potentials and corresponding variations of nodal space Na concentration. Single action potential (*A* and *B*) and train of action potentials elicited at a frequency of 100 Hz (*C* and *D*). $[Na]_s$ was calculated with the three-compartment model. The values of $P_{Na,s}$ and θ were, respectively, 0.0025 cm·s^{-1} and 0.3 μm (*A* and *C*) and 0.006 cm·s^{-1} and 0.058 μm (*B* and *D*). In *A*, the dashed line represents an action potential in the absence of Na depletion.

hypothesis in isotonic KCl Ringer's solution, in which a significant K accumulation can be detected in certain fibers for large depolarizations (Dubois, 1981*a*).

Modeling of Na Depletion During Computed Action Potential

In order to have an idea of the importance and the role of Na depletion, membrane action potentials were reconstructed on the basis of the model proposed by Frankenhaeuser and Huxley (1964). The Na depletion was calculated by using the three-compartment model in two extreme conditions: with the mean values of θ_{Na} and $P_{Na,s}$ calculated in normal fibers and with the corresponding values calculated in BTX-treated fibers. During action potentials, the Na

driving force and P_{Na} (calculated with the constant field equation) were continuously modified for changes in $[Na]_s$ induced by the Na current.

Fig. 15 presents single action potentials (*A* and *B*) and a train of action potentials elicited at a frequency of 100 Hz (*C* and *D*) and the corresponding changes in $[Na]_s$ calculated with $\theta_{Na} = 0.3$ μm and $P_{Na,s} = 0.0025$ cm·s^{-1} (*A* and *C*), and $\theta_{Na} = 0.058$ μm and $P_{Na,s} = 0.006$ cm·s^{-1} (*B* and *D*). In *A*, the dashed curve corresponds to an action potential calculated in the absence of Na depletion. Depending on the values of θ_{Na} and $P_{Na,s}$, $[Na]_s$ decreases from 114 to ~105 or 100 mM during a single action potential. During a train of action potentials, $[Na]_s$ decreases to ~90 mM with the values of θ_{Na} and $P_{Na,s}$ calculated in BTX-treated fibers (*C*). With the values of θ_{Na} and $P_{Na,s}$ calculated in normal fibers, the recovery of the resting $[Na]_s$ is almost complete between two action potentials, and the depletion induced by the first action potential is not increased further by the other action potentials. The decrease in $[Na]_s$, which can reach ~20% of the resting $[Na]_s$ (Fig. 15*C*), does not significantly influence either the duration of the action potential or its amplitude. Experimentally, we have observed that during a train of action potentials elicited at a frequency of 100 Hz in normal Ringer's solution, the second action potential and the following ones were ~7 mV smaller than the first one. Similar observations were made after blockade of K current by TEA (Dubois, 1981*b*). On the basis of the preceding model, this decrease in action potential amplitude is probably not due to Na depletion but is more likely to be due to Na inactivation.

DISCUSSION

The major findings in this report are: (*a*) Inward Na current induces a depletion of Na ions from the external surface of the nodal membrane both in BTX-treated and normal fibers. (*b*) The depletion of Na ions from the perinodal space induces not only a decrease in driving force for Na ions but also a decrease in Na conductance. After removal of the voltage-dependent inactivation by BTX, Na current and Na conductance present an apparent inactivation that is related to the decrease in Na concentration in the perinodal space ($[Na]_s$). (*c*) On the basis of a three-compartment model (Frankenhaeuser and Hodgkin, 1956), calculations of the space thickness (θ) and ionic permeability ($P_{I,s}$) of an apparent barrier between the space and the bulk solution indicate that θ is modified by ionic concentration changes in the space and that the barrier is more permeable to K than to Na. Changes in local ionic concentrations induced by ionic fluxes may play important roles in the activity of cells or neighboring cells, as already seen in the central nervous system. The three major findings reported above are discussed separately below.

Na Depletion from the Perinodal Space

The possibility of a decrease in Na concentration at the external surface of the nodal membrane during Na influx has been already suggested by Neumcke and Stämpfli (1983). A brief report by Scruggs and Narahashi (1983) indicated that Na depletion also exists in the space delimited by the Schwann cells and the axolemma in the squid giant axon. The present work represents the first

quantitative analysis of such a phenomenon. Several observations show that in normal or BTX-modified fibers, the reversal potential for Na current is modified by a predepolarization. The change in reversal potential can be due to a change either in local Na concentrations or in the selectivity of the channels (Mozhaeva et al., 1981). The observation that the change in reversal potential is directly proportional to the quantity of ions that have been displaced from one side of the membrane to the other during the predepolarization is in favor of changes in local ionic concentrations. Nevertheless, it must be noted that a part of the change in reversal potential can be related to changes in the selectivity of Na channels or to the existence of two types of Na channels with different ionic selectivities and kinetics. This conclusion is based upon the observations that during a depolarization near the reversal potential on normal fibers (Sigworth, 1981, Fig. 1) and on BTX-modified fibers (Dubois et al., 1983, Fig. 5), the TTX-sensitive current can exhibit successive inward and outward components. On BTX-treated fibers, this change in reversal potential seems to be related to the appearance of a second conductance component, which activates for depolarizations more positive than −50 mV (Dubois et al., 1983). Consequently, the change in reversal potential described here during depolarizations to −60 mV is probably related to changes in local ionic concentrations. In the central nervous system, the Na depletion during nerve cell activity may be of greater importance than in isolated node of Ranvier because nerve cells are tightly packed. In addition to direct effects on nerve excitability, Na depletion can greatly modify the metabolism of the cells by altering enzymatic activities and Na-coupled transport of metabolites.

Change in Na Conductance Induced by Na Depletion

The observation that during a voltage pulse the activated Na conductance declines almost linearly with the decrease in local Na concentration shows that the conductance can be modulated by transient Na concentration changes in the perinodal space and that the decrease in $[Na]_s$ decreases both the driving force and the conductance. These two phenomena contribute to a reduction in the current. In the node of Ranvier, this apparent inactivation is small, especially in normal fibers. However, it is quite possible that in other cells, a significant part of inward current inactivation may be due to a depletion of permeant ions from the external face of the membrane.

Properties of the Perinodal Space

The apparent barrier between the space and the bulk solution appears to be more permeable to K than to Na. This may be related to either selective bindings of ions with molecules located in the space or a selective K permeability of the Schwann cell membrane (see Pentreath, 1982). The perinodal space or nodal gap contains Schwann cell microvilli embedded in a polyanionic mucopolysaccharide nodal gap matrix substance with properties of cation exchanger (Langley, 1969, 1979). As suggested by Rydmark and Berthold (1983), the ions in the perinodal space may be sequestered by the matrix substance. However, it must be noted that, until now, ultrastructural morphometric analyses of the node of

Ranvier have been done almost exclusively in mammalian nerve fibers. Since the structure of amphibian and mammalian nodal gaps is different (M. Rydmark, personal communication), the properties of the gap substances in frog and mammalian node of Ranvier may be different. Nevertheless, the observation that the frog nodal gap matrix is apparently more permeable to K than to Na supports the view that the node-paranode apparatus may be involved in impulse transmission phenomena (Berthold and Rydmark, 1983).

Na depletion and K accumulation modify the space thickness (Fig. 14). If the space thickness, as calculated on the basis of Eq. 2, represents the thickness of the Schwann cells surrounding the fiber, the external diameter of the fibers should increase about two times in isotonic KCl Ringer's solution as compared with its value in normal Ringer's solution. Our own observation shows that this is not the case. After replacement of NaCl by KCl in the external solution, the diameter of the fiber may increase to some extent but certainly not twofold. This indicates that the space thickness (θ) is an apparent thickness corresponding to the distance that ions have to cover around the Schwann cell microvilli from the axolemma to the bulk solution or vice versa. In this case, θ is the product of the Schwann cell thickness by a tortuosity factor that corresponds to the folding of Schwann cells. During Na depletion or K accumulation, the increase in θ would be due mainly to an increase in tortuosity. This can be explained by a swelling of the Schwann cells. When $[K]_s$ increases, different permeabilities of the Schwann cell membrane for K and Cl, similar to those described in skeletal muscle (Zachar, 1971), may be responsible for an entry of KCl and water into Schwann cells, which consequently swell. When $[Na]_s$ decreases, a swelling of Schwann cells can be explained if one assumes that the osmotic pressure in the space tends to decrease and induces an entry of water into the Schwann cells.

These hypotheses imply that the Schwann cells play an important role in the control of external ionic concentrations. This conclusion, already proposed for the central nervous system (see review by Pentreath, 1982), also seems to be valid for peripheral nerves. During action potentials, Na depletion and K accumulation must develop almost simultaneously. The question arises as to whether both phenomena contribute to increasing θ. According to the hypotheses proposed above for the swelling of Schwann cells, the effects of Na depletion and K accumulation of θ must be cumulative. It would be of interest to test this prediction by calculations of θ_K in Ringer's solutions of various Na concentrations. It must be noted that such an experiment has already been carried out by Adelman et al. (1973) on the squid giant axon. These authors observed an increase in θ in 10% hyperosmotic artificial seawater (by addition of NaCl). This result apparently contradicts ours, but the experimental conditions were different.

We are indebted to Drs. J. Daly and B. Witkop for the supply of BTX. We are grateful to Dr. J. Tanguy for participating to preliminary experiments on normal fibers and to Profs. E. Coraboeuf and B. I. Khodorov for critical reading of the manuscript. We thank Mrs. P. Richer for her expert assistance in the preparation of the manuscript.

This work was supported in part by a grant from Ministère de l'Industrie et de la Recherche (France) (No. 83 C 0329).

Received for publication 17 August 1983 and in revised form 23 January 1984.

REFERENCES

Adelman, W. J., Y. Palti, and J. P. Senft. 1973. Potassium ion accumulation in a periaxonal space and its effects on the measurement of membrane potassium ion conductance. *J. Membr. Biol.* 13:387–410.

Adrian, R. H., W. K. Chandler, and A. L. Hodgkin. 1970. Voltage clamp experiments in striated muscle fibres. *J. Physiol. (Lond.).* 208:607–644.

Baumgarten, C. M., and G. Isenberg. 1977. Depletion and accumulation of potassium in the extracellular clefts of cardiac Purkinje fibers during voltage clamp hyperpolarization and depolarization. *Pflügers Arch. Eur. J. Physiol.* 368:19–31.

Baylor, D. A., and J. G. Nicholls. 1969. Changes in extracellular K^+ concentration produced by neuronal activity in the central nervous system of the leech. *J. Physiol. (Lond.).* 203:555–569.

Bergman, C. 1970. Increase of sodium concentration near the inner surface of nodal membrane. *Pflügers Arch. Eur. J. Physiol.* 317:287–302.

Berthold, C.-H., and M. Rydmark. 1983. Electron microscopic serial section analysis of nodes of Ranvier in lumbosacral spinal roots of the cat. Ultrastructural organization of nodal compartments in fibres of different sizes. *J. Neurocytol.* 12:475–505.

Chiu, S. Y. 1977. Inactivation of sodium channels: second order kinetics in myelinated nerve. *J. Physiol. (Lond.).* 273:573–596.

Cleemann, L., and M. Morad. 1979*a*. Extracellular potassium accumulation in voltage-clamped frog ventricular muscle. *J. Physiol. (Lond.).* 286:83–111.

Cleemann, L., and M. Morad. 1979*b*. Potassium currents in frog ventricular muscle: evidence from voltage clamp currents and extracellular K accumulation. *J. Physiol. (Lond.).* 286:113–134.

Cohen, I., and R. Kline. 1982. K^+ fluctuations in the extracellular spaces of cardiac muscle. Evidence from the voltage clamp and extracellular K^+ selective microelectrodes. *Circ. Res.* 50:1–16.

Connors, B. W., B. R. Ransom, D. M. Kunis, and M. J. Gutnick. 1982. Activity-dependent K^+ accumulation in the developing rat optic nerve. *Science (Wash. DC).* 216:1341–1343.

De Bruin, G. 1982. Conditioning prepulses and kinetics of potassium conductance in the frog node. *J. Membr. Biol.* 70:27–35.

Dubois, J. M. 1981*a*. Simultaneous changes in the equilibrium potential and potassium conductance in voltage clamped Ranvier node in the frog. *J. Physiol. (Lond.).* 318:279–295.

Dubois, J. M. 1981*b*. Properties and physiological roles of K^+ currents in frog myelinated nerve fibres as revealed by 4-aminopyridine. *In* Advances in the Biosciences. Vol. 35: Aminopyridines and Similarly Acting Drugs. P. Lechat, S. Thesleff, and W. C. Bowman, editors. Pergamon Press, New York. 43–51.

Dubois, J. M., and C. Bergman. 1971. Conductance sodium de la membrane nodale: inhibition compétitive calcium-sodium. *C. R. Acad. Sci. Paris Ser. D.* 272:2924–2927.

Dubois, J. M., and C. Bergman. 1975. Potassium accumulation in the perinodal space of frog myelinated axons. *Pflügers Arch. Eur. J. Physiol.* 358:111–124.

Dubois, J. M., and M. F. Schneider. 1981. Effect of oenanthotoxin on sodium current and intra-membrane charge movement in frog node of Ranvier. *Adv. Physiol. Sci.* 4:79–87.

Dubois, J. M., M. F. Schneider, and B. I. Khodorov. 1983. Voltage dependence of intramem-

brane charge movement and conductance activation of batrachotoxin-modified sodium channels in frog node of Ranvier. *J. Gen. Physiol.* 81:829–844.

Frankenhaeuser, B., and A. L. Hodgkin. 1956. The after-effects of impulses in the giant nerve fibres of *Loligo*. *J. Physiol. (Lond.)*. 131:341–376.

Frankenhaeuser, B., and A. F. Huxley. 1964. The action potential in the myelinated nerve fibre of *Xenopus laevis* as computed on the basis of voltage clamp data. *J. Physiol. (Lond.)*. 171:302–315.

Goldman, D. E. 1943. Potential, impedance and rectification in membrane. *J. Gen. Physiol.* 27:37–70.

Hodgkin, A. L., and B. Katz. 1949. The effect of sodium ions on the electrical activity of the giant axon of the squid. *J. Physiol. (Lond.)*. 108:37–77.

Khodorov, B. I., E. M. Peganov, S. V. Revenko, and L. D. Shishkova. 1975. Sodium currents in voltage clamped nerve fibre of frog under the combined action of batrachotoxin and procaine. *Brain. Res.* 84:541–546.

Khodorov, B. I., and S. V. Revenko. 1979. Further analysis of the mechanisms of action of batrachotoxin on the membrane of myelinated nerve. *Neuroscience*. 4:1315–1330.

Kline, R. P., I. Cohen, R. Falk, and J. Kupersmith. 1980. Activity-dependent extracellular K^+ fluctuations in canine Purkinje fibres. *Nature (Lond.)*. 286:68–71.

Landowne, D., and V. Scruggs. 1981. Effects of internal and external sodium on the sodium current-voltage relationship in the squid giant axon. *J. Membr. Biol.* 59:79–89.

Langley, O. K. 1969. Ion-exchange at the node of Ranvier. *Histochem. J.* 1:295–309.

Langley, O. K. 1979. Histochemistry of polyanions in peripheral nerve. *In* Complex Carbohydrates of Nervous Tissue. R. U. Margolis and R. K. Margolis, editors. Plenum Press, New York. 193–207.

Moran, N., Y. Palti, E. Levitan, and R. Stämpfli. 1980. Potassium ion accumulation at the external surface of the nodal membrane in frog myelinated fibers. *Biophys. J.* 32:939–954.

Mozhaeva, G. N., A. P. Naumow, and B. I. Khodorov. 1981. Changes in properties of Na channels in the nodal membrane treated with batrachotoxin (BTX). USSR-Sweden III Symposium on Physico-Chemical Biology Abstracts. 221–222.

Neher, E., and H. D. Lux. 1973. Rapid changes of potassium concentration at the outer surface of exposed single neurons during membrane current flow. *J. Gen. Physiol.* 61:385–399.

Neumcke, B., and R. Stämpfli. 1983. Alteration of the conductance of Na^+ channels in the nodal membrane of frog nerve by holding potential and tetrodotoxin. *Biochim. Biophys. Acta.* 727:177–184.

Noble, S. J. 1976. Potassium accumulation and depletion in frog atrial muscle. *J. Physiol. (Lond.)*. 258:579–613.

Nonner, W. 1969. A new voltage clamp method for Ranvier nodes. *Pflügers Arch. Eur. J. Physiol.* 309:116–192.

Nonner, W., E. Rojas, and R. Stämpfli. 1975. Displacement currents in the node of Ranvier. Voltage and time dependence. *Pflügers Arch. Eur. J. Physiol.* 354:1–18.

Pentreath, V. W. 1982. Potassium signalling of metabolic interaction between neurons and glial cells. *Trends Neurosci.* 5:339–345.

Rydmark, M., and C.-H. Berthold. 1983. Electron microscopic serial section analysis of nodes of Ranvier in lumbar spinal roots of the cat. A morphometric study of nodal compartments in fibres of different sizes. *J. Neurocytol.* 12:537–565.

Scruggs, V., and T. Narahashi. 1983. Accumulation and depletion of Na ions in the periaxonal space of the squid giant axon. *Biophys. J.* 41:55*a*. (Abstr.)

Sigworth, F. J. 1981. Covariance of nonstationary sodium current fluctuations at the node of Ranvier. *Biophys. J.* 34:111–133.

Somjen, G. G. 1979. Extracellular potassium in the mammalian central nervous system. *Annu. Rev. Physiol.* 41:159–177.

Zachar, J. 1971. Electrogenesis and Contractility in Skeletal Muscle Cells. University Park Press, Baltimore and London. 1–638.